Comparative label-free proteomic analysis of equine osteochondrotic chondrocytes

Journal of Proteomics 228 (2020) 103927

Contents lists available at ScienceDirect

Journal of Proteomics

journal homepage: www.elsevier.com/locate/jprot

Comparative label-free proteomic analysis of equine osteochondrotic chondrocytes

Elisabetta Chiaradia[a,*], Marco Pepe[a,*], Paola Sassi[b], Ronny Mohren[c], Pier Luigi Orvietani[d], Marco Paolantoni[b], Alessia Tognoloni[a], Monica Sforna[a], Maxime Eveque[c], Niki Tombolesi[b], Berta Cillero-Pastor[c]

[a] Department of Veterinary Medicine, University of Perugia, via San Costanzo 4, 06126 Perugia, Italy
[b] Department of Chemistry, Biology and Biotechnology, University of Perugia, via Elce di sotto 8, 06123 Perugia, Italy
[c] The Maastricht Multimodal Molecular Imaging Institute (M4I), Division of Imaging Mass Spectrometry, Maastricht University, The Netherlands
[d] Department of Experimental Medicine, University of Perugia, via Gambuli, 1, 06132 Perugia, Italy

ARTICLE INFO

Keywords:
Osteochondrosis
Chondrocytes
Proteomics
Raman spectroscopy
Cartilage

ABSTRACT

Osteochondrosis is a developmental orthopedic disease affecting growing cartilage in young horses. In this study we compared the proteomes of equine chondrocytes obtained from healthy and osteochondrotic cartilage using a label-free mass spectrometry approach. Quantitative changes of some proteins selected for their involvement in different functional pathways highlighted by the bioinformatics analysis, were validated by western blotting, while biochemical alterations of extracellular matrix were confirmed via Raman spectroscopy analysis. In total 1637 proteins were identified, of which 59 were differentially abundant. Overall, the results highlighted differentially represented proteins involved in metabolic and functional pathways that may be related to the failure of the endochondral ossification process occurring in osteochondrosis. In particular, we identified proteins involved in extracellular matrix degradation and organization, vitamin metabolism, osteoblast differentiation, apoptosis, protein folding and localization, signalling and gene expression modulation and lysosomal activities. These results provide valuable new insights to elucidate the underlying molecular mechanisms associated with the development and progression of osteochondrosis.

Significance: Osteochondrosis is a common articular disorder in young horses mainly due to defects in endochondral ossification. The pathogenesis of osteochondrosis is still poorly understood and only a limited number of proteomic studies have been conducted. This study provides a comprehensive characterization of proteomic alterations occurring in equine osteochondrotic chondrocytes, the only resident cell type that modulates differentiation and maturation of articular cartilage. The results evidenced alterations in abundance of proteins involved in functional and metabolic pathways and in extracellular matrix remodelling. These findings could help clarify some molecular aspects of osteochondrosis and open new fields of research for elucidating the pathogenesis of this disease.

1. Introduction

Osteochondrosis (OC) is a developmental orthopedic disease characterized by the failure of normal cartilage maturation [1–4]. It is one of the most common articular disorders in growing horses with a very high incidence rate (10–70%) [2], depending on the breed as well as nutritional and genetic factors which may have serious consequences for animal health and welfare [5–8]. OC has been described in several animal species including dogs, cattle, pigs and humans with similar hallmarks [8]. Although, many hypotheses on the etiopathogenesis of OC have been proposed, such as rapid growth, genetic predisposition, trauma and nutrition, it is still poorly understood [1,6,9–12].

OC could be interpreted as failure of the transition from the cartilaginous matrix to skeletal maturity during skeletal growth, mainly due to the complex cellular events that involve chondrocytes [1,3,5]. These cells play a significant role in cartilage homeostasis by modulating extracellular matrix (ECM) turnover and mineralization. Structural changes in cartilage and subchondral bone, such as fissures, bone cysts, attached or free-floating cartilage fragments in the joint cavity, are typical features of OC [1,2,7,9,13]. The presence of fragments that

* Corresponding authors.
E-mail addresses: elisabetta.chiaradia@unipg.it (E. Chiaradia), marco.pepe@unipg.it (M. Pepe).

https://doi.org/10.1016/j.jprot.2020.103927
Received 26 February 2020; Received in revised form 16 July 2020; Accepted 28 July 2020
Available online 05 August 2020
1874-3919/

classify this pathology as osteochondrosis dissecans (OCD), may cause joint inflammation that may evolve into osteoarthritis (OA) [1,6,14,15].

Several proteomic studies have already been carried out to improve the understanding of the physiopathology of joint diseases such as OA, rheumatoid arthritis (RA) and juvenile idiopathic arthritis [16–22], however few studies have focused on the proteomic analysis of OC [23–28]. Chondrocytes are the unique cartilage cell type and therefore playing an important role in bone growth and elongation and promote ECM remodelling and replacement. However, the only proteomic study on OC chondrocytes was performed using a two-dimensional electrophoresis (2DE)-based approach [24].

The aim of the present study was to provide further information on the cellular and molecular mechanisms underlying OC pathogenesis. For this purpose, a differential proteomic analysis of healthy and OC chondrocytes using a label-free mass spectrometry-based protein quantification strategy was performed. This approach provides a more comprehensive description of the proteome alterations in OC cells, overcoming the limits of gel-based analysis used in the previous study. Proteins showing a significantly differential abundance between OC and healthy chondrocytes, were functionally annotated using bioinformatic tools in order to highlight the metabolic and functional pathways associated with the disease. Quantitative changes of some proteins were validated using western blotting. Raman spectroscopy (RS) was used to confirm the biochemical composition changes of OC cartilage. Indeed, RS has recently revealed biomolecular features and distribution of collagens and glycosaminoglycans in cartilage tissue that cannot be accurately evidenced by conventional radiography and computed tomography [29,30]. This study provides new insights into the molecular mechanisms of OC and aims at finding new management approaches and innovative therapeutic strategies to improve equine health and welfare.

2. Materials and methods

2.1. Cartilage and chondrocyte harvesting

Equine chondrocytes were isolated from cartilage samples collected from the metacarpal/metatarsophalangeal joints of 14 male thoroughbred race horses (1–4 years old, 7 with OC and 7 without joint diseases, respectively). In short, the OC cells were obtained from OC osteochondral fragments collected during arthroscopy from clinical cases referred to the University of Perugia Veterinary Teaching Hospital, in accordance with the guidelines issued by the Animal Care and Use Committee of the University of Perugia. In particular, five fragments were obtained from proximal sagittal ridge lesions of third metacarpal/metatarsal bones (MCIII/MTIII) and two from dorsoproximal aspect of proximal phalanx. The racehorse owners signed written informed consent for the samples used in this study and the diagnoses were determined using radiography and arthroscopy (Fig. 1 A and B). The traumatic origin of fragments was excluded based on their OC radiographic appearance and on the anamnestic data/history of horses included in the study (none of animals enrolled were involved in training or in racing). The control (CTR) cells were isolated from normal articular cartilage obtained from animals euthanized for other medical reasons. The control joints were selected based on the absence of macroscopic abnormalities, typical clinical features of joint diseases (OC or OA) and microscopic alterations. Typical histological features of normal cartilage were evidenced in hematoxylin and eosin (HE)-stained, formalin-fixed, paraffin-embedded samples of healthy cartilage [31] (Fig. 1D).

Cartilage samples (7 OC and 7 CTR) were individually used to obtain chondrocytes. Slices were harvested under sterile conditions, using sterile scalpels, rinsed twice in Dulbecco's phosphate-buffered saline (DPBS) (Sigma-Aldrich Corp, St. Louis, USA) containing penicillin (100 U/mL), streptomycin (100 mg/mL) and amphotericin B (250 μg/mL) [32]. Minced cartilage slices were then incubated with trypsin (0.25%) at 37 °C for 10 min and then with collagenase type I (2 mg/mL) (Sigma-Aldrich Corp.) at 37 °C for 8–10 h. The chondrocytes were separated from undigested tissue cells using a 70 μm cell strainer (BD Biosciences Inc., San Jose, USA). After washing in DPBS, the cells were resuspended in low glucose Dulbecco's modified Eagle's medium (DMEM) (Sigma-Aldrich Corp.) and supplemented with 10% fetal bovine serum (Sigma-Aldrich Corp.), penicillin (100 U/mL) and streptomycin (100 μg/mL). The cells were then placed into cell culture flasks at the density of 2×10^4 cells/cm^2 and incubated at 37 °C in a 5% CO_2 humidified atmosphere. Monolayer cells were expanded until confluent and then detached using trypsin/EDTA (0.25%) (Sigma-Aldrich, Corp.), washed three times and kept at −80 °C until analysis. Subculture passages were avoided in order to minimize phenotype changes.

2.2. Proteomic analysis

2.2.1. Protein extraction

Condrocytes from each cell culture (7 OC and 7 CTR) were analyzed. All samples were individually collected in 5 M Urea (GE Healthcare, Chicago, USA) and 50 mM Ammonium bicarbonate (ABC) (GE Healthcare). Cell lysis was performed by three freeze-thaw cycles, using a − 80 °C freezer and approximately 40 s of sonication in an ultrasonic bath. Total protein concentration was determined by Bradford assay (Bio-Rad Hercules, USA), according to the manufacturer's instructions.

2.2.2. In solution digestion

Protein samples were reduced with 20 mM Dithiothreitol (DTT) (GE Healthcare) for 45 min and alkylated with 40 mM Iodoacetamide (IAM) (GE Healthcare) for 45 min in darkness. The alkylation was stopped by adding 30 mM DDT. Digestion was performed with a mixture of LysC and Trypsin (Promega, Madison, USA), which was added at a ratio of 1:25 (enzyme to protein). After two hours of digestion at 37 °C in a Thermo Shaker (Grant Instruments, Royston. UK) at 250 rpm, the lysate was diluted with 50 mM ABC to 1 M Urea and further digested at 37 °C, 250 rpm, overnight. The digestion was terminated by adding formic acid (FA) (Biosolve, Valkenswaard, NL) to a total of 1%.

2.2.3. Ultra high-performance liquid chromatography (UHPLC) and label-free mass spectrometry (MS)

Peptide separation was performed on a Thermo Scientific Ultimate 3000 Rapid Separation UHPLC system (Dionex, Amsterdam, NL) equipped with a PepSep C18 analytical column (15 cm, ID 75 μm, 1,9 μm Reprosil, 120 Å). Peptide samples were first desalted on an online installed C18 trapping column. After desalting, peptides were separated on the analytical column with a 90 min linear gradient from 5% to 35% Acetonitrile (ACN) (Biosolve) with 0.1% FA at 300 nL/min flow rate. The UHPLC system was coupled to a Q Exactive HF mass spectrometer (Thermo Fisher Scientific, San Jose, USA). Data dependent acquisition (DDA) settings were as follows: Full MS scan between 250 and 1250 *m/z* at resolution of 120,000 followed by MS/MS scans of the top 15 most intense ions at a resolution of 15,000.

2.2.4. Mass spectrometry data analysis

For protein identification and quantitation the spectra were analyzed with Proteome Discoverer (PD) version 2.2. Within the PD software, the search engine Sequest was used with the SwissProt [*Human*] database (*Homo sapiens* (SwissProt TaxID = *9606*)) and SwissProt [*Horse*] database (*Equus caballus* (SwissProt TaxID = 9796)).

The database search was performed with the following settings: Enzyme trypsin, a maximum of 2 missed cleavages, minimum peptide length of 6, precursor mass tolerance of 10 ppm, fragment mass tolerance of 0.02 Da, dynamic modifications of methionine oxidation and protein N-terminus acetylation, fixed modification of cysteine carbamidomethylation. Only proteins with false discovery rate (FDR) ≤ 1%

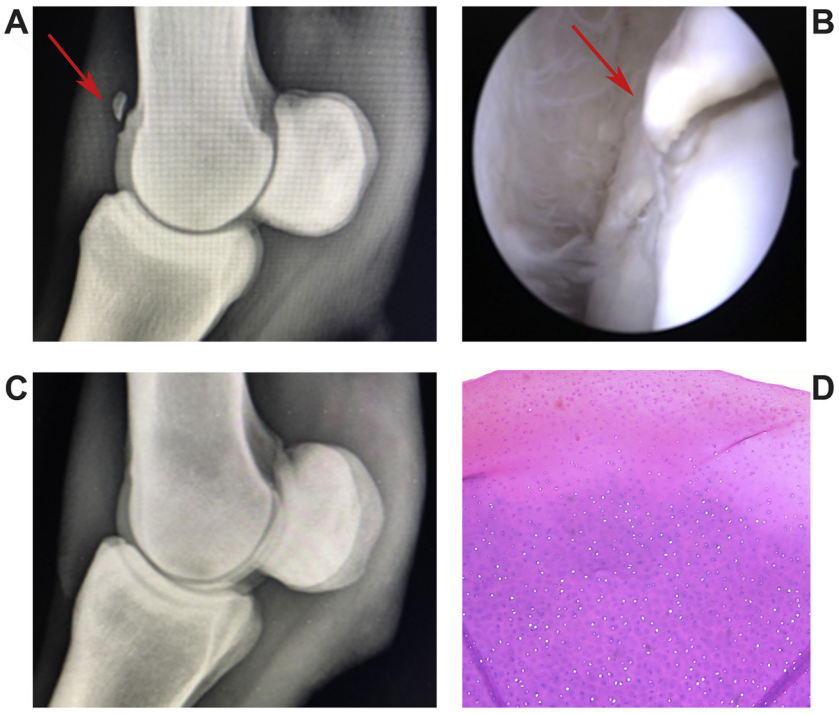

Fig. 1. Representative images of healthy (CTR) and osteochondrotic (OC) joints and healthy cartilage. A) Radiographic image of metacarpo-phalangeal joint (latero-medial view) with OC fragment (indicated by the red arrow) of the proximal aspect of sagittal ridge of the third metacarpal bone (MCIII). B) Arthroscopic image of the proximal aspect of the sagittal ridge of MCIII with OC fragment indicated by the red arrow. C) Radiographic image of normal metacarpo-phalangeal joint (Latero-medial view), D) Histological features of normal cartilage (hematoxylin and eosin-magnification 40×). (For interpretation of the references to colour in this figure legend, the reader is referred to the web version of this article.)

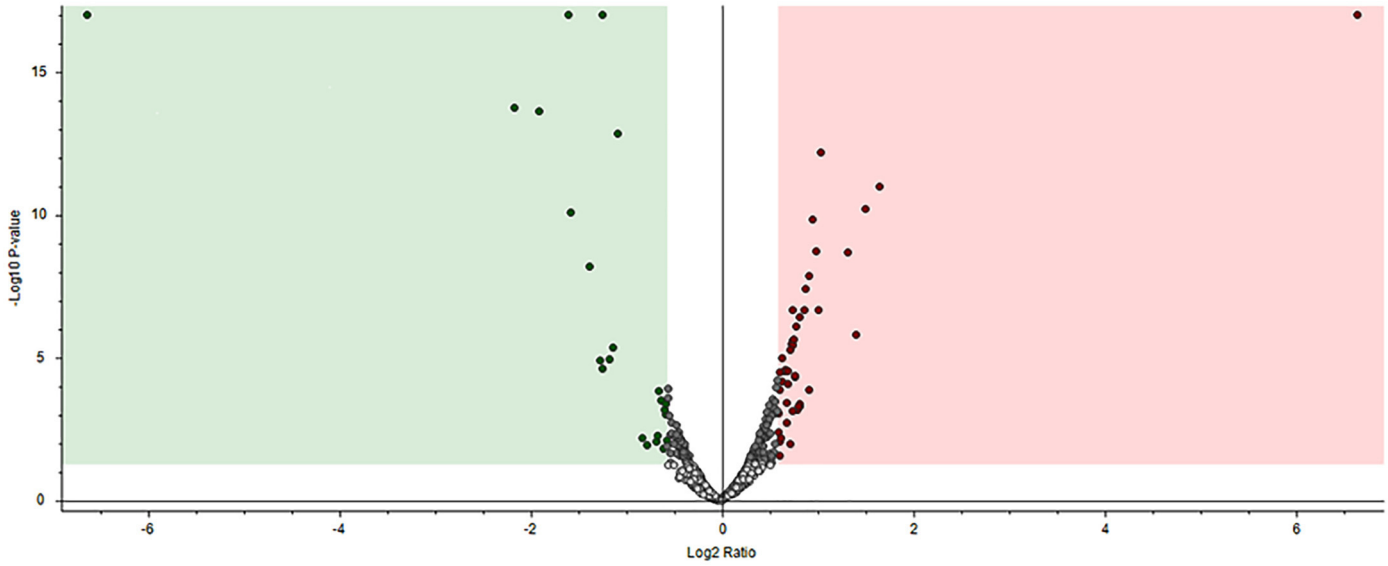

Fig. 2. Volcano plot showing differentially abundant proteins in osteochondrotic (OC) vs healthy (CTR) equine chondrocytes. The $-\log_{10}$ (p value) is plotted vs the $\log_2$ (fold change: OC/CTR). The dots above the non-axial horizontal line represent proteins with significantly different abundances ($p < 0.05$). Dots to the left of the non-axial vertical line represent protein fold changes of OC/CTR lower than -1.5, while dots to the right of the non-axial vertical line correspond to protein fold changes of OC/CTR with differences greater than 1.5. Significantly less and more abundant proteins ($p < 0.05$) are plotted in green and red respectively. (For interpretation of the references to colour in this figure legend, the reader is referred to the web version of this article.)

were considered as confident identifications and subjected to subsequent data analysis.

Protein quantitation was performed by using default Label Free Quantitation (LFQ) settings in Proteome Discoverer 2.2. In short, for peptide abundancies the peptide precursor intensities were used and normalization was performed on total peptide amount. Protein ratios were calculated based on pairwise peptide ratios and background-based ANOVA was used for hypothesis testing. Benjamini-Hochberg correction for multiple testing was used to calculate adjusted p-values. Proteins that were defined as differentially abundant were those with a $\geq$ 1.5 fold change and with a FDR adjusted p value of ≤ 0.05.

2.3. Bioinformatic analysis

Functional annotation and Network analysis were performed using STRING software (http://string-db.org/) and Cytoscape platform version 3.7.2 (https://cytoscape.org) using human orthologous genes. In particular, the two plugins of Cytoscape, namely Cluego and Clupedia [33,34] were used to integrate the GO categories (Biological Process (BP), Molecular Function (MF), Cellular Component (CC)), Reactome Pathways, Kyoto Encyclopedia of Genes and Genomes (KEGG), and Wiki Pathways annotation. The κ score level was set at ≥ 0.4 while minimum and maximum levels were set at 3 and 8, respectively.

Table 1
Differentially abundant proteins in osteochondrotic (OC) and healthy (CTR) equine chondrocytes. Gene and protein names, molecular weight (MW), fold change (OC/CTR) and *p* value (Benjamini-Hochberg corrected) are listed.

Gene name	Protein name	MW (kDa)	Fold change	*p*-Value
ACTA1	Actin, alpha skeletal muscle	42	1.7	$2.48e^{-05}$
LMNA	Isoform C of Prelamin-A/C	65.1	1.5	$4.66e^{-03}$
SOD2	Superoxide dismutase [Mn], mitochondria	24.7	1.9	$1.18e^{-06}$
FBN1	Fibrillin-1	312	1.9	$3.02e^{-06}$
GSN	Gelsolin O	80.8	1.6	$1.18e^{-03}$
DPYSL3	Isoform LCRMP-4 of Dihydropyrimidinase-related protein 3	73.9	2.0	$1.08e^{-10}$
CAT	Catalase	59.7	1.5	$2.75e^{-03}$
FAP	prolyl endopeptidase FAP	87.7	1.6	$2.78e^{-04}$
AP1B1	AP-1 complex subunit beta-1	104.6	1.6	$3.30e^{-03}$
UCHL1	Ubiquitin carboxyl-terminal hydrolase isozyme	24.9	1.7	$1.99e^{-04}$
CTSD	Cathepsin D	44.5	1.8	$1.39e^{-04}$
FTH1	Ferritin heavy chain	21.3	1.5	$5.19e^{-04}$
MYLK	Myosin light chain kinase, smooth muscle	210.6	2	$1.72e^{-07}$
ITGA11	Isoform 2 of Integrin alpha-11	133.5	1.6	$1.27e^{-03}$
TAGLN3	Transgelin-3	22.5	2.66	$9.42e^{-05}$
RBP1	Isoform 3 of Retinol-binding protein 1	17.5	1.6	$1.27e^{-03}$
DNM1	Dynamin-1	97.3	100	$2.1e^{-15}$
PLBD2	Putative phospholipase B-like	65.4	1.7	$1.5e^{-05}$
ZYX	Zyxin	61.2	1.5	$2.08e^{-02}$
CYP1B1	Cytochrome P450 1B1	60.8	1.5	$1.29e^{-03}$
TPP1	Tripeptidyl-peptidase 1	61.2	1.9	$1.58e^{-08}$
HEXA	Beta-hexosaminidase subunit alpha	60.7	1.7	$1.96e^{-03}$
SNX18	Sorting nexin-18	68.9	1.7	$4.97e^{-05}$
GAA	lysosomal alpha-glucosidase	105.3	1.8	$1.5e^{-05}$
MMP13	Collagenase 3	54.2	100	$2.1e^{-15}$
DNAJC8	DnaJ homolog subfamily C member 8	29.8	1.7	$1.49e^{-04}$
CBFB	Isoform 2 of Core-binding factor subunit beta	22	1.6	$1.23e^{-02}$
PDLIM2	Isoform 5 of PDZ and LIM domain protein 2	62.7	1.7	$1.67e^{-03}$
PZP	Pregnancy zone protein	163.8	1.9	$4.83e^{-03}$
H1F0	Histone H1.0	20.9	2.09	$1.47e^{-05}$
HEXB	Beta-hexosaminidase subunit beta	63.1	1.79	$1.30e^{-02}$
FOLR2	Folate receptor beta	29.3	1.69	$1.96e^{-04}$
FBLIM1	Isoform 2 of Filamin-binding LIM protein 1	40.3	1.7	$2.06e^{-02}$
FOLR1	Folate receptor alpha	29.8	1.7	$1.44e^{-02}$
CPM	Carboxypeptidase M	50.5	2.5	$1.91e^{-07}$
COMMD3	COMM domain-containing protein 3	22.1	1.7	$1.85e^{-02}$
HTRA1	Serine protease HTRA1	51.3	1.7	$1.52e^{-02}$
AGA	N(4)-(beta-*N*-acetylglucosaminyl)-L-asparaginase	37.2	2.8	$8.27e^{-09}$
S100A13	Protein S100-A13	11.5	1.5	$2.42e^{-02}$
HMOX1	heme oxygenase 1	32.8	1.6	$4.16e^{-02}$
PDLIM3	PDZ and LIM domain protein 3	39.2	3.1	$1.36e^{-09}$
TPM3	Tropomyosin alpha-3 chain	32.9	0.2	$3.62e^{-12}$
COL1A1	Collagen alpha-1(I) chain	138.9	0.6	$1.02e^{-02}$
STMN1	Isoform 2 of Stathmin	19.8	0.6	$2.58e^{-02}$
RBBP7	Isoform 2 of Histone-binding protein RBBP7	52.3	0.6	$1.25e^{-02}$
FABP5	Fatty acid-binding protein, epidermal	15.2	0.6	$5.21e^{-03}$
CTHRC1	Collagen triple helix repeat-containing protein 1	26.2	0.6	$1.91e^{-02}$
HMGCS1	hydroxymethylglutaryl-CoA synthase, cytoplasmic	57.3	0.3	$2.1e^{-15}$
DDX50	ATP-dependent RNA helicase DDX50	82.5	0.4	$6.07e^{-04}$
SERPINE1	Plasminogen activator inhibitor 1	45	0.4	$2.1e^{-15}$
DUT	Deoxyuridine 5′-triphosphate nucleotidohydrolase, mitochondrial	26.5	0.3	$1.02e^{-08}$
PPP3R1	Calcineurin subunit B type 1	19.3	0.4	$2.28e^{-04}$
CRABP2	Cellular retinoic acid-binding protein 2	15.7	0.4	$5.34e^{-04}$
KPNA2	Importin subunit alpha-1	57.8	0.4	$5.54e^{-07}$
MBD3	methyl-CpG-binding domain protein 3	32.8	0.01	$2.1e^{-15}$
SSR1	Translocon-associated protein subunit alpha	32.2	0.4	$2.35e^{-11}$
SKIL	Ski-like protein	76.9	0.3	$4.15e^{-12}$
PRUNE2	Isoform 3 of Protein prune homolog 2	340.9	0.4	$1.13e^{-03}$
ALCAM	CD166 antigen	65.1	0.01	$2.1e^{-15}$

2.4. Western blotting

Immunoblotting was performed to validate the findings of the mass spectrometry-based quantitative proteomic analysis. The proteins extracted from OC and CTR cells were mixed in six pools (3 OC and 3 CTR, same quantity of each sample), separated by SDS-PAGE 10% or 12%, depending on the molecular mass of protein under evaluation) and blotted on PDVF membranes. The blotted membranes were incubated with antibodies against actin (ACT) (Sigma-Aldrich, 1:5000), beta-hexosaminidase subunit beta (HEXB) (Santa Cruz, 1:1000), mitochondrial superoxide dismutase (SOD2), (Cell Signaling, 1:5000), collagenase 3 (MMP13) (Santa Cruz, 1:1000), cytochrome P450 1B1 (CYP1B1) (Santa Cruz, 1:1000), catalase (CAT) (Abcam, 1:2000) and tubulin (TUB) (Santa Cruz, 1:5000) at 4 °C overnight and then with the appropriate anti-mouse HRP secondary antibody (Sigma-Aldrich, 1:5000) or anti-rabbit HRP secondary antibody (Sigma-Aldrich 1:5000). Immunoreactivity was detected by chemiluminescence using the ECL system (Bio-Rad). Images were acquired using a GS-800 imaging systems scanner (Bio-Rad). A densitometric analysis was performed with Quantity One 4.5.0 software (Bio-Rad) using tubulin bands as

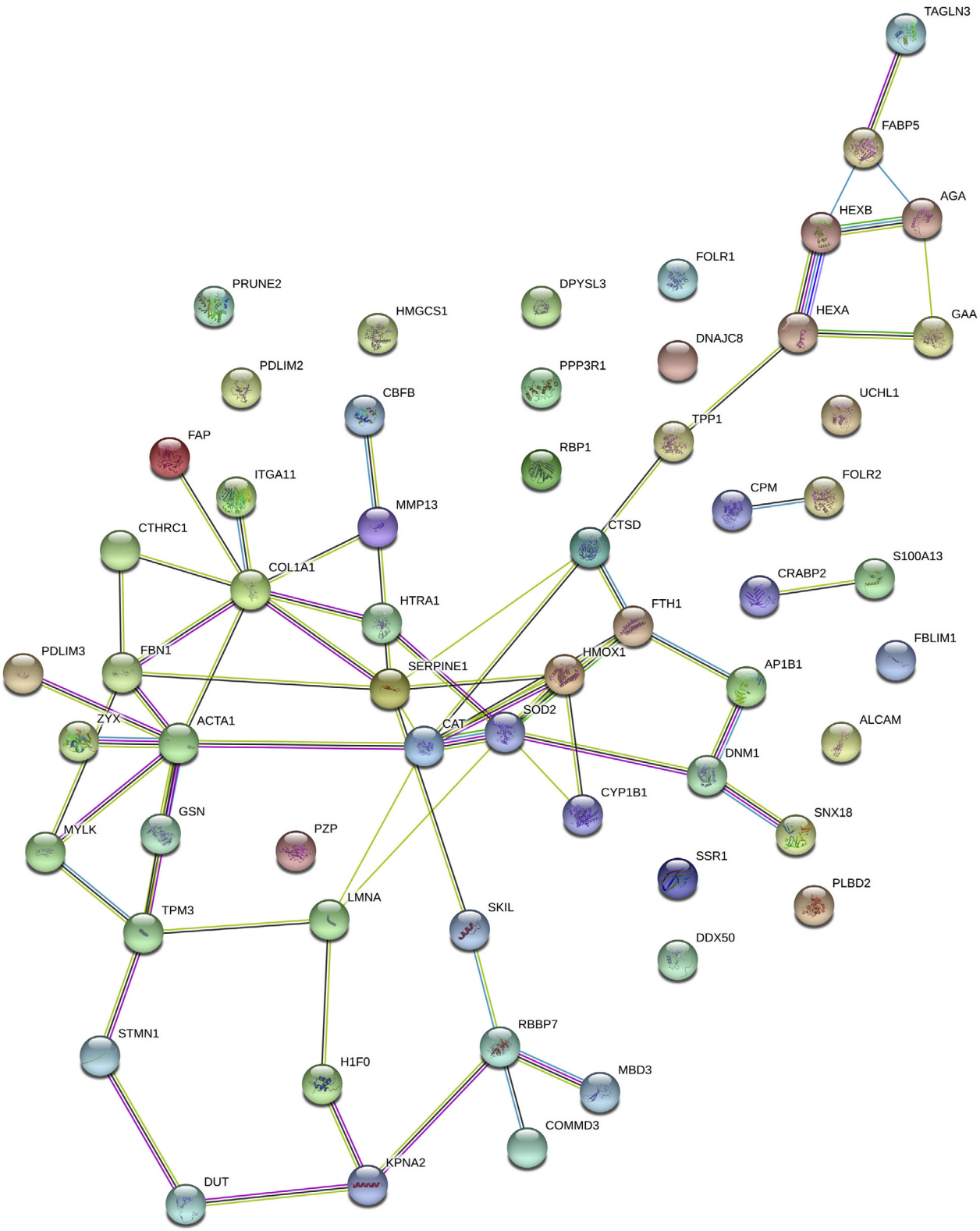

Fig. 3. STRING Protein Protein Interaction (PPI) analysis. PPI analysis of differentially abundant proteins in osteochondrotic (OC) vs healthy (CTR) equine chondrocytes. p-value = $2.22e^{-09}$. Gene name of proteins are reported.

normalization factor. The *t*-test was carried out for the statistical analysis where $p \leq 0.05$ was considered significant.

2.5. Raman spectroscopy

Cartilage samples were embedded in OCT prior to cryosectioning, cut (Leica CM1900 Cryostat) at 10 μm and mounted on a silicon substrate. Raman spectra were collected using a micro-Raman setup

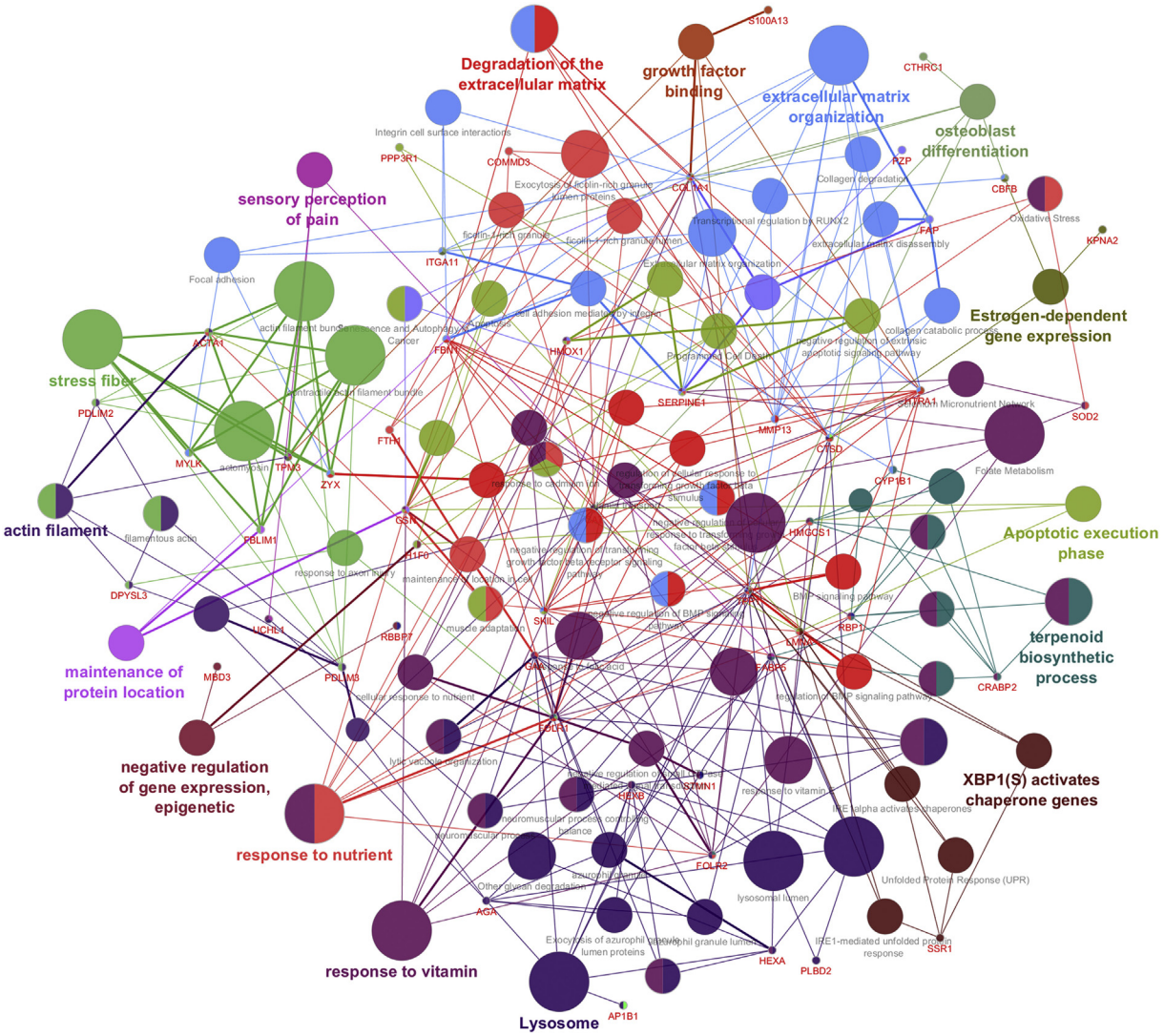

Fig. 4. Functionally grouped network analysis of differentially abundant proteins in osteochondrotic (OC) vs healthy (CTR) equine chondrocytes. Biological process, molecular function, cellular component, Reactome, Kyoto Encyclopedia of Genes and Genomes (KEGG), and WikiPathway have been integrated to perform analysis. (A) Terms as nodes linked were analyzed based on their kappa score level (≥ 0.4), where only the label of the most significant term per group is shown.

equipped with a solid-state laser at $\lambda = 532$ nm. Power was maintained at 8 mW to reduce photon damage to the samples during acquisition. A back-scattering geometry was realized using the 50× long working distance objective of an OLYMPUS microscope MOD BX40, equipped with a digital camera HORIBA, model Syncerity. The scattered radiation was analyzed by an iHR320 imaging spectrometer Horiba Jobin-Yvon. The signal was dispersed by a 1800 grooves/mm grating which allowed spectra acquisition in the 600–1720 cm^{-1} range. Spectra were recorded as an average of 10 scans, each one accumulated within 60s integration time, using at 5 cm^{-1} resolution.

3. Results

3.1. Proteomic analysis

The quantitative label free MS-based proteomic analysis identified 1637 proteins, of which 59 resulted as differentially abundant (fold change ≥ 1.5, p-value ≤ 0.05) in OC compared to CTR chondrocytes. In particular, 18 proteins were less-abundant in OC chondrocytes compared to CTR samples whereas 41 were upregulated in the OC condition. These results are shown in a volcano plot (Fig. 2), while the list of the differentially abundant proteins is reported in Table 1. Data corresponding to MS identification and quantitation are listed in supplementary table 1 (Table S1).

3.2. Functional enrichment and interaction network analysis

An overview of the protein-protein interactions (PPI) was generated by Search Tool for the Retrieval of Interacting Genes (STRING). The PPI analysis of proteins that were differentially showed in OC (Fig. 3) evidenced an interactome consisting of 59 nodes, 64 edges, 2.17 average node degree, 0.357 average local clustering coefficient and 28 expected edges. The PPI enrichment p-value was $2.22e^{-09}$. The gene ontology (GO) analysis by String revealed that the main CC categories were: “Lysosome” including 12 proteins, “extracellular region” including 23 proteins, “stress fiber” with 5 proteins and others that are listed in Table S2 with the corresponding FDR. The most significant BP categories were “system development” with 31 proteins, “anatomical structure morphogenesis” including 20 proteins, “anatomical structure development” including 34 proteins and “cellular component organization” with 33 proteins (Table S2) .

The statistically significant ($p < 0.05$) network analysis performed using Cytoscape is shown in Fig. 4 and listed in Table S3. In particular, the main functional groups included “degradation of extracellular

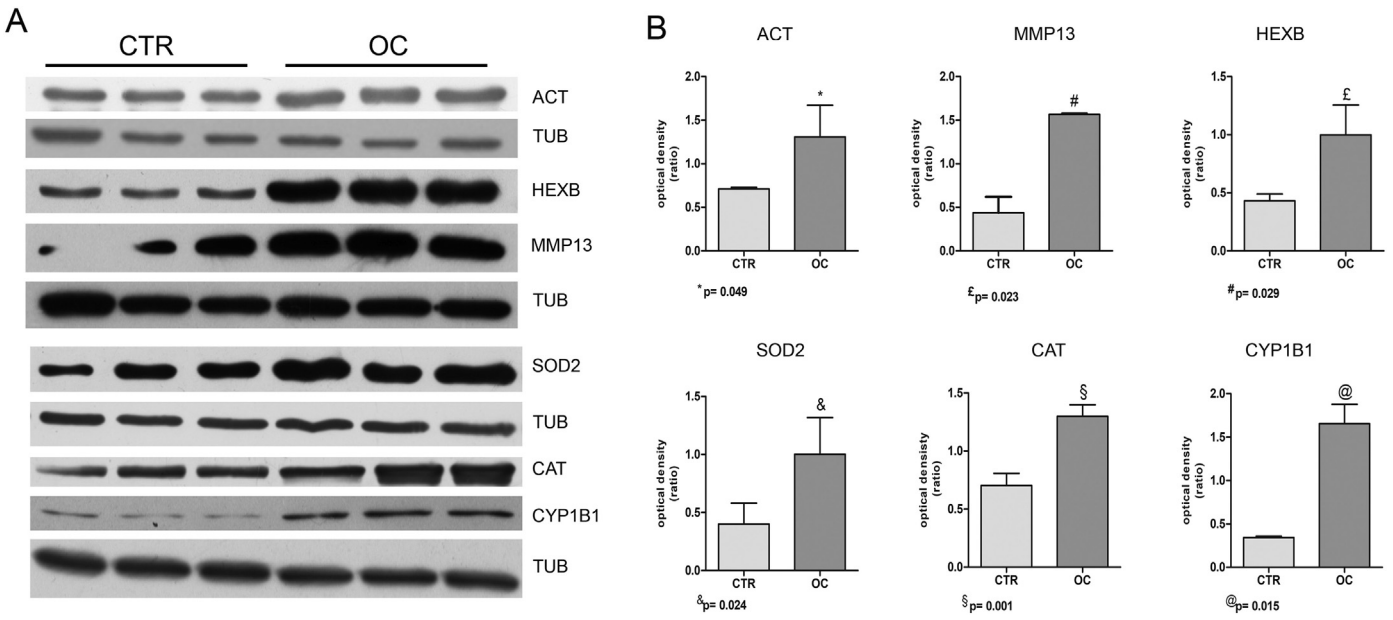

Fig. 5. Western Blotting to validate label-free quantitation results. Western blotting of proteins obtained from osteochondrotic (OC) and healthy chondrocytes (CTR) was performed using antibodies against actin (ACT), beta-hexosaminidase subunit beta (HEXB), collagenase 3 (MMP13) mitochondrial superoxide dismutase (SOD2), cytochrome P450 1B1 (CYP1B1) and catalase (CAT). Tubulin (TUB) was used as housekeeping. A) Representative images; B) Bar graph showing normalized western blotting band densities. Data represent the mean ± SEM of three independent experiments.

matrix" and "extracellular matrix organization" indicating structural and functional ECM alterations. Moreover, "lysosome" and "exopeptidase activity" pathways evidenced a high hydrolase activity. "Maintenance of protein location" and "XPB1 (S) activates chaperone gene" indicated deregulation of protein folding and localization. Among the most significant terms were also "osteoblast differentiation", "apoptotic execution phase" and "growth factor binding" that reflected changes in cell differentiation and cell death. Finally response to vitamin" and "response to nutrient" were also evidenced.

3.3. Western blotting

In order to verify the results of the label-free based proteomic analysis, some proteins of interest were further validated using western blotting. The candidate proteins were selected based on their involvement in various functional categories or pathways highlighted by the bioinformatic analysis. ACT, HEXB and MMP13 were analyzed to confirm the cytoskeletal, lysosomal and ECM alteration respectively. Western blotting of SOD2, CYP1B1 and CAT were performed in order to validate the involvement of oxidative stress in OC (Fig. 5). As shown in Fig. 5A and B the results confirmed the increase of all tested proteins.

3.4. Raman spectroscopy

The results of the label-free quantification approach were further corroborated by RS. The spectra (Fig. 6) showed significant differences in the relative intensities of collagen and GAG bands that indicate a reduction in GAG content, as well as alterations in collagen fiber structure and organization in OC tissues.

4. Discussion

Proteomics has, to date, been poorly applied to study the pathogenesis of OC. In this study we carried out a comparative proteomic analysis of equine chondrocytes obtained from healthy and OC cartilage using a label-free MS approach.

Overall, we identified differentially abundant proteins involved in metabolic and functional pathways that may be related to endochondral ossification failure in OC. This may confirm the osteochondrotic nature of the analyzed fragments. Indeed, there is still much the debate on the different origins of joint fragments, especially when they occur within the fetlock joints [35,36].

In particular, the results indicated structural and functional ECM modifications and cytoskeletal alterations which have direct consequences on cell adhesion. Some proteins involved in cell death and differentiation, as well as in gene expression, were also modulated. Moreover, the results confirmed the role of nutrition in OC pathogenesis and highlighted a probable involvement of lysosomal enzymes. According to previous studies [24,25] the deregulation of proteins involved in endoplasmic reticulum stress response and protein folding and localization were also observed.

The key steps of the endochondral ossification process consisting in the conversion of cartilage ECM into natural bone ECM [37] seem to have been highly compromised. Indeed, proteins related to the "degradation of extracellular matrix" and "extracellular matrix organization" were identified. Moreover, the RS analysis of OC cartilage, also showed alterations in ECM consisting of modifications in collagen protein structure, collagen fiber disorganization and GAG degradation. Changes in collagen content may be due to the elevated MMP13 levels revealed by our analysis and previously described in OC lesions [38–40] as well as to the low level of collagen type 1 content observed in the OC cells. ECM remodelling may also have been affected by alterations in the ratio serine proteases/serine protease inhibitors that are essential for ECM turnover [41]. In fact our results showed a drop in the serpine 1 protein level, which is a serine protease inhibitor that plays a key role in chondrogenesis, cartilage and bone remodelling [42]. Furthermore, large amounts of two serine proteases were observed, namely prolyl-endopeptidase a cell surface glycoprotein with collagenase and gelatinase activities, and serine protease HTRA1 that hydrolyses ECM proteins such as fibronectin, fibromodulin and proteoglycans (PGs). ECM abnormalities can also be caused by lysosomal enzymes. In the OC cells, we detected a high abundance of beta-hexosaminidase subunit alpha and beta (HEXA - HEXB), lysosomal alpha-glucosidase, N(4)-(beta-*N*-acetylglucosaminyl)-L-asparaginase and cathepsin D. These enzymes are involved in cartilage turnover [43]. Although initially PG degradation occurs extracellularly, fragments are endocytosed and

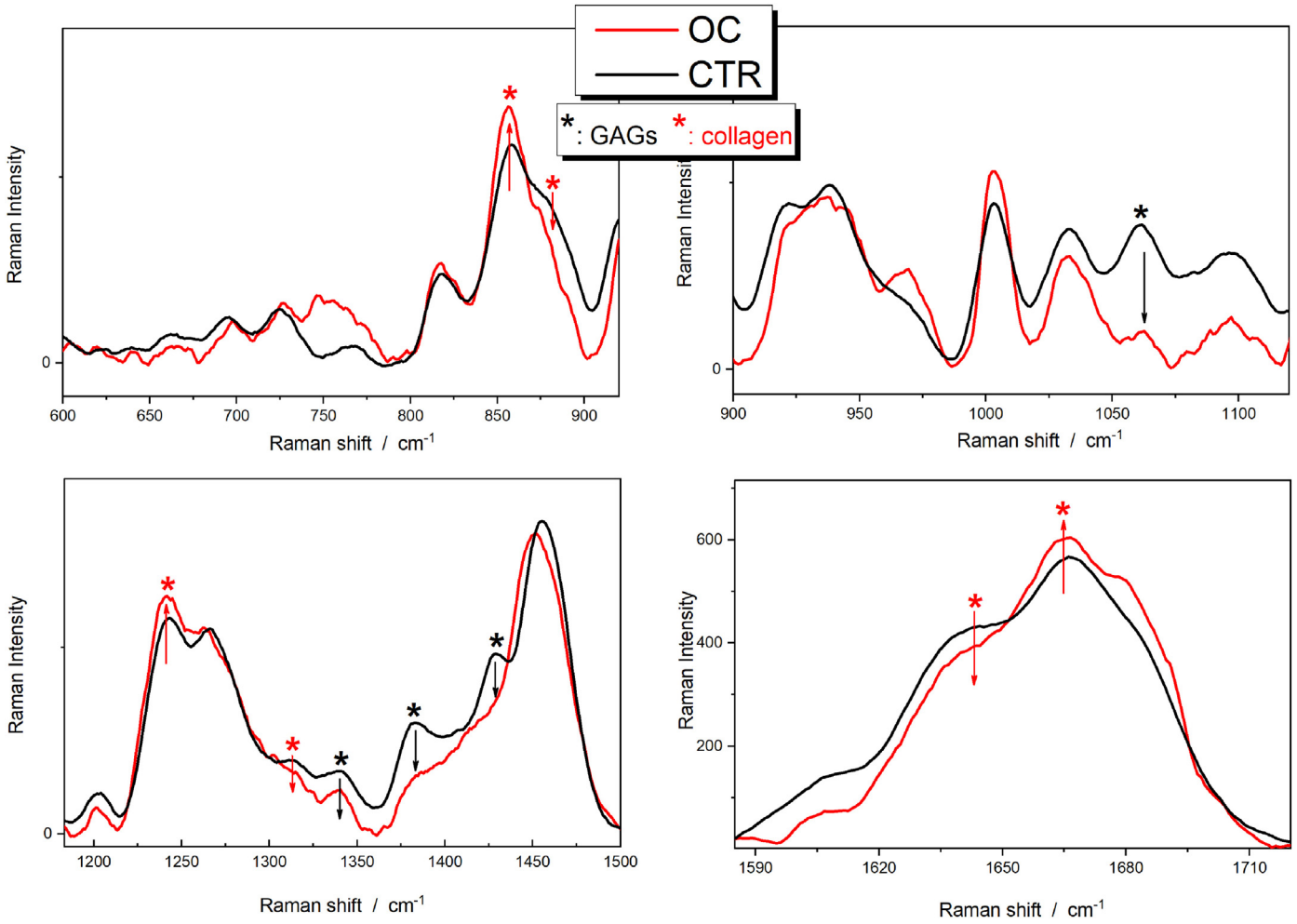

Fig. 6. Raman spectra of healthy (CTR) and osteochondrotic (OC) cartilage. Raman spectra of cartilage samples in the 600–1720 cm^{-1} region. Characteristic bands of GAGs ad collagen are marked with the black and red asterisks, respectively. (For interpretation of the references to colour in this figure legend, the reader is referred to the web version of this article.)

subjected to further hydrolysis in lysosomes. Moreover, chondrocyte lysosomal exocytosis occurs and lysosomal hydrolases such as cathepsin D and β-hexosaminidase can degrade extracellular PGs during endochondral ossification [44]. Moreover, cathepsin D was found to be differentially distributed in osteochondrotic cartilage [45]. Another possible role of lysosomes in OC pathogenesis might also be linked to their involvement in autophagy that could be triggered in the growth plate chondrocytes during endochondral ossification [46]. The overactivation of autophagy and apoptosis, such as evidenced in the present study are both proposed and still debated to promote chondrocytes cell-death [47]. Moreover, our functional analysis annotated some deregulated proteins also in the “apoptosis execution phase”.

In accordance with our previous study [24], changes in the abundance of cytoskeletal proteins were detected. In addition to the high levels of actin, herein alterations were observed in abundance of proteins included in cytoskeletal structures such as “actin filament” and “stress fiber”. These proteins regulate the chondrocyte phenotype and the mechanotransduction mechanisms with direct implications in cartilage homeostasis and pathology [48]. Alterations in actin dynamics, cellular architecture, cell adhesion and integrin signalling, may be also due to the deregulation of isoform 5 of PDZ and LIM domain protein 2, PDZ and LIM domain protein 3, filamin-binding LIM 1 and zyxin protein levels [49–52]. Cytoskeletal alterations could be also caused to a drop in stathmin, also known as OP18, which is a key endogenous regulator of microtubule dynamism. It plays a role in metabolism and bone homeostasis by promoting osteoblast differentiation and inhibiting osteoclast formation [53].

The role of nutrition in OC pathogenesis [54–57] was confirmed, as alterations in “response to vitamin” and “response to nutrient” were evidenced. In particular, changes in the amounts of the retinol binding protein 1 (RBP1) and cellular retinoic acid-binding protein (CRABP2) were observed as well as in folate receptor beta (FOLR2) and folate receptor alpha (FOLR1). RBP1 and CRABP2 are key elements of the retinoid signalling pathway which is essential for skeletal development and growth [58,59]. FOLR2 and FOLR1 transport folic acids which are required for chondrocyte differentiation [60] and for one carbon metabolism [61].

The cytoscape analysis confirmed the role of growth factors and epigenetics that have already been suggested in cartilage maturation and in endochondral ossification but poorly investigated in OC [2,3,62,63]. Furthermore “estrogen-dependent gene expression” seems to be compromised. Although little is known about the role of estrogens in OC, they are able to directly affect chondrocyte proliferation and differentiation, ECM collagens and PG content, as well as differentiation and apoptosis of osteoblasts and osteoclasts [64,65]. Moreover, our results also revealed alterations in “osteoblast differentiation” that could be significantly affected by reduction in collagen triple helix repeat-containing protein 1 (CTHRC1) in OC chondrocytes. CTHRC1 is involved in the crosstalk between osteoblasts and osteoclasts [66] and in the Wnt pathway which is a key regulator of joint remodelling [67].

Furthermore, the results suggested a possible role for bone morphogenetic protein (BMP) signalling in OC, which has been poorly

investigated. Indeed, the "XBP1(S) activates chaperone genes" emerged as another signalling pathway deregulated in OC cells. The spliced X-box binding protein 1 isoform (XBP1s) is a key inducer in the BMP2 signalling pathway, involved in chondrogenesis and bone formation as well as in osteoblast differentiation and extracellular matrix mineralization [68–70].

Finally, impairment of OC chondrocyte homeostasis may also be due to highly reactive oxygen species (ROS) levels and pro-oxidant conditions, which could promote an antioxidant cellular response, thus confirming the role of oxidative stress in OC [14]. Indeed, our results showed an increased abundance of oxidative stress-related proteins such as catalase, SOD2, CYP1B1 and heme oxygenase 1 (HMOX1). In mammalian cells, CYP1B1, a member of Cytochrome P450 enzyme family is one of the two main endogenous sources of ROS and the main inducer of pro-oxidant conditions [71,72]. Moreover, SOD 2, catalase and HMOX1 expression are induced by the nuclear transcription factor erythroid 2-related factor 2, which coordinates the response to oxidative stress stimulating the synthesis of antioxidant enzymes [73].

5. Conclusions

This study identified differentially abundant proteins that could be key players in the onset and progression of osteochondrosis. In particular, lysosome-associated proteins and proteins that are involved in ECM organization and degradation, cell adhesion, vitamin metabolism and osteoblast differentiation were detected. Overall, these findings could open new fields of research aimed at clarifying the OC pathogenesis as alterations were observed in some proteins associated with endochondral ossification. Finally, the results could be translated to other species as the pathogenesis of OC is shared across different species and equine OCD is a good animal model for human juvenile OCD.

Supplementary data to this article can be found online at https://doi.org/10.1016/j.jprot.2020.103927.

Declaration of Competing Interest

The authors declare no competing financial interest.

Acknowledgements

This work has been performed as part of the M4I research program that was financially supported by the Dutch Province of Limburg through the "LINK" program and the MUMC institutional grant for clinical collaborative research.

Author contributions

Elisabetta Chiaradia: Conceptualization, Methodology, Data curation, Validation, Writing- Original draft preparation, Performing the experiments. Paola Sassi: Conceptualization, Methodology, Data curation, Writing- Reviewing and Editing, specifically RS analysis. Marco Pepe: Conceptualization, Methodology, Writing- Reviewing and Editing, Supervision. Ronny Mohren: Conducting a research and investigation process, specifically performing the experiments of MS analysis. Pier Luigi Orvietani: Conducting a research and investigation process, specifically performing the experiments of WB. Marco Paolantoni: Conceptualization, Methodology, Data curation, Writing-Reviewing and Editing, specifically RS analysis. Alessia Tognoloni: Conducting a research and investigation process, specifically performing the experiments of WB and cell culture. Maxime Eveque: Conducting a research and investigation process, specifically performing the experiments of MS analysis. Monica Sforna: Conducting a research and investigation process, specifically performing histological examination of cartilage. Niki Tombolesi: Conducting a research and investigation process, specifically performing the experiments of RS analysis. Berta Cillero Pastor: Conceptualization, Methodology, Data curation, Reviewing and Editing, Supervision. All authors have given approval to the final version of the manuscript.

References

[1] B. Ytrehus, C.S. Carlson, S. Ekman, Etiology and pathogenesis of osteochondrosis, Vet. Pathol. 44 (2007) 429–448, https://doi.org/10.1354/vp.44-4-429.
[2] P.R. van Weeren, L.B. Jeffcott, Problems and pointers in osteochondrosis: twenty years on, Vet. J. 197 (2013) 96–102, https://doi.org/10.1016/j.tvjl.2013.03.048.
[3] S.A. Semevolos, Osteochondritis dissecans development, Vet. Clin. North Am. Equine Pract. 33 (2017) 367–378, https://doi.org/10.1016/j.cveq.2017.03.009.
[4] P.R. van Weeren, K. Olstad, Pathogenesis of osteochondrosis dissecans: how does this translate to management of the clinical case? Equine Vet. Educ. 28 (2016) 155–166, https://doi.org/10.1111/eve.12435.
[5] R. van Weeren, Fifty years of osteochondrosis, Equine Vet. J. 50 (2018) 554–555, https://doi.org/10.1111/evj.12821.
[6] J.T. Bates, J.C. Jacobs, K.G. Shea, J.T. Oxford, Emerging genetic basis of osteochondritis dissecans, Clin. Sports Med. 33 (2014) 199–220, https://doi.org/10.1016/j.csm.2013.11.004.
[7] K. Olstad, S. Ekman, C.S. Carlson, An update on the pathogenesis of Osteochondrosis, Vet. Pathol. 52 (2015) 785–802, https://doi.org/10.1177/0300985815588778.
[8] A.M. McCoy, F. Toth, N.I. Dolvik, S. Ekman, J. Ellermann, K. Olstad, B. Ytrehus, C.S. Carlson, Articular osteochondrosis: a comparison of naturally-occurring human and animal disease, Osteoarthr. Cartil. 21 (2013) 1638–1647, https://doi.org/10.1016/j.joca.2013.08.011.
[9] S. Laverty, C. Girard, Pathogenesis of epiphyseal osteochondrosis, Vet. J. 197 (2013) 3–12, https://doi.org/10.1016/J.TVJL.2013.03.035.
[10] L. Vander Heyden, J.P. Lejeune, I. Caudron, J. Detilleux, C. Sandersen, P. Chavatte, J. Paris, B. Deliège, D. Serteyn, Association of breeding conditions with prevalence of osteochondrosis in foals, Vet. Rec. 172 (2013) 68, https://doi.org/10.1136/vr.101034.
[11] G.S. Maier, D. Lazovic, U. Maus, K.E. Roth, K. Horas, J.B. Seeger, Vitamin D deficiency: the missing etiological factor in the development of juvenile osteochondrosis dissecans? J. Pediatr. Orthop. 39 (2019) 51–54, https://doi.org/10.1097/BPO.0000000000000921.
[12] F. Naccache, J. Metzger, O. Distl, Genetic risk factors for osteochondrosis in various horse breeds, Equine Vet. J. 50 (2018) 556–563, https://doi.org/10.1111/evj.12824.
[13] S.A. Semevolos, Osteochondritis dissecans development, Vet. Clin. North Am. Equine Pract. 33 (2017) 367–378, https://doi.org/10.1016/j.cveq.2017.03.009.
[14] L. Bourebaba, M. Röcken, K. Marycz, Osteochondritis dissecans (OCD) in horses – molecular background of its pathogenesis and perspectives for progenitor stem cell therapy, Stem Cell Rev. Rep. 15 (2019) 374–390, https://doi.org/10.1007/s12015-019-09875-6.
[15] F. Al-Hizab, P.D. Clegg, C.C. Thompson, S.D. Carter, Microscopic localization of active gelatinases in equine osteochondritis dissecans (OCD) cartilage, Osteoarthr. Cartil. 10 (2002) 653–661, https://doi.org/10.1053/joca.2002.0811.
[16] S. Mun, J. Lee, A. Park, H.-J. Kim, Y.-J. Lee, H. Son, M. Shin, M.-K. Lim, H.-G. Kang, Proteomics approach for the discovery of rheumatoid arthritis biomarkers using mass spectrometry, Int. J. Mol. Sci. 20 (2019), https://doi.org/10.3390/ijms20184368.
[17] Y.-J. Park, M.K. Chung, D. Hwang, W.-U. Kim, Proteomics in rheumatoid arthritis research, Immune Netw. 15 (2015) 177–185, https://doi.org/10.4110/in.2015.15.4.177.
[18] M.F. Hsueh, P. Önnerfjord, V.B. Kraus, Biomarkers and proteomic analysis of osteoarthritis, Matrix Biol. 39 (2014) 56–66, https://doi.org/10.1016/j.matbio.2014.08.012.
[19] A. Mobasheri, Applications of proteomics to osteoarthritis, a musculoskeletal disease characterized by aging, Front. Physiol. 2 (2011) 108, https://doi.org/10.3389/fphys.2011.00108.
[20] S.M. Mahendran, K. Oikonomopoulou, E.P. Diamandis, V. Chandran, Synovial fluid proteomics in the pursuit of arthritis mediators: an evolving field of novel biomarker discovery, Crit. Rev. Clin. Lab. Sci. 54 (2017) 495–505, https://doi.org/10.1080/10408363.2017.1408561.
[21] C. Ruiz-Romero, P. Fernández-Puente, V. Calamia, F.J. Blanco, Lessons from the proteomic study of osteoarthritis, Expert Rev. Proteomics. 12 (2015) 433–443, https://doi.org/10.1586/14789450.2015.1065182.
[22] V. Trachana, E. Mourmoura, I. Papathanasiou, A. Tsezou, Understanding the role of chondrocytes in osteoarthritis: utilizing proteomics, Expert Rev. Proteomics. 16 (2019) 201–213, https://doi.org/10.1080/14789450.2019.1571918.
[23] J.R. Anderson, A. Smagul, D. Simpson, P.D. Clegg, L.M. Rubio-Martinez, M.J. Peffers, The synovial fluid proteome differentiates between septic and non-septic articular pathologies, J. Proteome 202 (2019) 103370, , https://doi.org/10.1016/j.jprot.2019.04.020.
[24] E. Chiaradia, M. Pepe, P.L. Orvietani, G. Renzone, A. Magini, M. Sforna, C. Emiliani, A. Di Meo, A. Scaloni, Proteome alterations in equine Osteochondrotic chondrocytes, Int. J. Mol. Sci. 20 (2019), https://doi.org/10.3390/ijms20246179.
[25] C. Desjardin, S. Chat, M. Gilles, R. Legendre, J. Riviere, X. Mata, T. Balliau, D. Esquerré, E.P. Cribiu, J.-M. Betch, L. Schibler, Involvement of mitochondrial dysfunction and ER-stress in the physiopathology of equine osteochondritis dissecans (OCD), Exp. Mol. Pathol. 96 (2014) 328–338, https://doi.org/10.1016/j.yexmp.2014.03.004.
[26] C. Desjardin, J. Riviere, A. Vaiman, C. Morgenthaler, M. Diribarne, M. Zivy, C. Robert, L. Le Moyec, L. Wimel, O. Lepage, C. Jacques, E. Cribiu, L. Schibler, Omics technologies provide new insights into the molecular physiopathology of equine osteochondrosis, BMC Genomics 15 (2014) 947, https://doi.org/10.1186/

1471-2164-15-947.
[27] R. Liu, L. Fan, L. Yin, K. Wang, W. Miao, Q. Song, X. Dang, H. Gao, C. Bai, Comparative study of serum proteomes in Legg-calve-Perthes disease, BMC Musculoskelet. Disord. 16 (2015) 281, , https://doi.org/10.1186/s12891-015-0730-z.
[28] E. Chiaradia, M. Pepe, M. Tartaglia, F. Scoppetta, C. D'Ambrosio, G. Renzone, L. Avellini, F. Moriconi, A. Gaiti, A. Bertuglia, F. Beccati, A. Scaloni, Gambling on putative biomarkers of osteoarthritis and osteochondrosis by equine synovial fluid proteomics, J. Proteomics. 75 (2012). doi:https://doi.org/10.1016/j.jprot.2012.02.008.
[29] M.S. Bergholt, A. Serio, M.B. Albro, M.B. Albro, Raman spectroscopy: guiding light for the extracellular matrix, front, Bioeng. Biotechnol. 7 (2019) 1–16, https://doi.org/10.3389/fbioe.2019.00303.
[30] C.D. Hosu, V. Moisoiu, A. Stefancu, E. Antonescu, L.F. Leopold, N. Leopold, D. Fodor, Raman spectroscopy applications in rheumatology, Lasers Med. Sci. 34 (2019) 827–834, https://doi.org/10.1007/s10103-019-02719-2.
[31] N. Schmitz, S. Laverty, V.B. Kraus, T. Aigner, Basic methods in histopathology of joint tissues, Osteoarthr. Cartil. (2010), https://doi.org/10.1016/j.joca.2010.05.026.
[32] F. Mancini, S. Nannarone, S. Buratta, G. Ferrara, A.M. Stabile, M. Vuerich, I. Santinelli, A. Pistilli, E. Chiaradia, Effects of xylazine and dexmedetomidine on equine articular chondrocytes in vitro, Vet. Anaesth. Analg. 44 (2017), https://doi.org/10.1016/j.vaa.2016.04.004.
[33] G. Bindea, B. Mlecnik, H. Hackl, P. Charoentong, M. Tosolini, A. Kirilovsky, W.H. Fridman, F. Pagès, Z. Trajanoski, J. Galon, ClueGO: a cytoscape plug-in to decipher functionally grouped gene ontology and pathway annotation networks, Bioinformatics. 25 (2009) 1091–1093, https://doi.org/10.1093/bioinformatics/btp101.
[34] G. Bindea, J. Galon, B. Mlecnik, CluePedia cytoscape plugin: pathway insights using integrated experimental and in silico data, Bioinformatics. 29 (2013) 661–663, https://doi.org/10.1093/bioinformatics/btt019.
[35] B. O'Meara, Osteochondrosis dissecans of the fetlock joint – diagnosis, management and prognosis, Livestock. 21 (2016) 262–267, https://doi.org/10.12968/live.2016.21.4.262.
[36] J. Declercq, A. Martens, D. Maes, B. Boussauw, R. Forsyth, K.J. Boening, Dorsoproximal proximal phalanx osteochondral fragmentation in 117 warmblood horses, Vet. Comp. Orthop. Traumatol. 22 (2009) 1–6, https://doi.org/10.3415/VCOT-08-02-0016.
[37] C.H.A. Van De Lest, P.A.J. Brama, B. Van El, J. Degroot, P.R. Van Weeren, Extracellular matrix changes in early osteochondrotic defects in foals: a key role for collagen? Biochim. Biophys. Acta Mol. Basis Dis. 1690 (2004) 54–62, https://doi.org/10.1016/j.bbadis.2004.05.002.
[38] M. Mirams, L. Tatarczuch, Y.A. Ahmed, C.N. Pagel, L.B. Jeffcott, H.M.S. Davies, E.J. Mackie, Altered gene expression in early osteochondrosis lesions, J. Orthop. Res. 27 (2009) 452–457, https://doi.org/10.1002/jor.20761.
[39] M. Mirams, B.A. Ayodele, L. Tatarczuch, F.M. Henson, C.N. Pagel, E.J. Mackie, Identification of novel osteochondrosis–associated genes, J. Orthop. Res. 34 (2016) 404–411, https://doi.org/10.1002/jor.23033.
[40] T.L. Riddick, K. Duesterdieck-Zellmer, S.A. Semevolos, Gene and protein expression of cartilage canal and osteochondral junction chondrocytes and full-thickness cartilage in early equine osteochondrosis, Vet. J. 194 (2012) 319–325, https://doi.org/10.1016/j.tvjl.2012.04.023.
[41] D.J. Wilkinson, M.D.C. Arques, C. Huesa, A.D. Rowan, Serine proteinases in the turnover of the cartilage extracellular matrix in the joint: implications for therapeutics, Br. J. Pharmacol. 176 (2019) 38–51, https://doi.org/10.1111/bph.14173.
[42] D.J. Wilkinson, M. del C. Arques, C. Huesa, A.D. Rowan, Serine proteinases in the turnover of the cartilage extracellular matrix in the joint: implications for therapeutics, Br. J. Pharmacol. 176 (2019) 38–51, https://doi.org/10.1111/bph.14173.
[43] J. Popko, S. Olszewski, T. Guszczyn, K. Zwierz, S. Pancewicz, Glycoconjugate markers of joint diseases, Biochem. Soc. Trans. (2011) 331–335, https://doi.org/10.1042/BST0390331.
[44] E.R. Bastow, K. Last, S. Golub, J.L. Stow, A.C. Stanley, A.J. Fosang, Evidence for lysosomal exocytosis and release of aggrecan-degrading hydrolases from hypertrophic chondrocytes, in vitro and in vivo, Biol. Open. 1 (2012) 318–328, https://doi.org/10.1242/bio.2012547.
[45] G. Hernandez-Vidal, L.B. Jeffcott, M.E. Davies, Cellular heterogeneity in cathepsin D distribution in equine articular cartilage, Equine Vet. J. 29 (1997) 267–273, https://doi.org/10.1111/j.2042-3306.1997.tb03122.x.
[46] P. Luo, F. Gao, D. Niu, X. Sun, Q. Song, C. Guo, Y. Liang, W. Sun, The role of autophagy in chondrocyte metabolism and osteoarthritis: a comprehensive research review, Biomed. Res. Int. 2019 (2019), https://doi.org/10.1155/2019/5171602.
[47] E.J. Mackie, Y.A. Ahmed, L. Tatarczuch, K.-S. Chen, M. Mirams, Endochondral ossification: how cartilage is converted into bone in the developing skeleton, Int. J. Biochem. Cell Biol. 40 (2008) 46–62, https://doi.org/10.1016/j.biocel.2007.06.009.
[48] E.J. Blain, Involvement of the cytoskeletal elements in articular cartilage homeostasis and pathology, Int. J. Exp. Pathol. 90 (2009) 1–15, https://doi.org/10.1111/j.1365-2613.2008.00625.x.
[49] J. Krcmery, T. Camarata, A. Kulisz, H.-G. Simon, Nucleocytoplasmic functions of the PDZ-LIM protein family: new insights into organ development, Bioessays. 32 (2010) 100–108, https://doi.org/10.1002/bies.200900148.
[50] G. Li, X. Song, R. Li, L. Sun, X. Gong, C. Chen, L. Yang, Zyxin-involved actin regulation is essential in the maintenance of vinculin focal adhesion and chondrocyte differentiation status, Cell Prolif. 52 (2019) e12532, , https://doi.org/10.1111/cpr.12532.
[51] R.F. Loeser, Integrins and chondrocyte-matrix interactions in articular cartilage, Matrix Biol. 39 (2014) 11–16, https://doi.org/10.1016/j.matbio.2014.08.007.
[52] G. Xiao, H. Cheng, H. Cao, K. Chen, Y. Tu, S. Yu, H. Jiao, S. Yang, H.J. Im, D. Chen, J. Chen, C. Wu, Critical role of filamin-binding LIM protein 1 (FBLP-1)/migfilin in regulation of bone remodeling, J. Biol. Chem. 287 (2012) 21450–21460, https://doi.org/10.1074/jbc.M111.331249.
[53] H. Liu, R. Zhang, S.Y. Ko, B.O. Oyajobi, C.J. Papasian, H.W. Deng, S. Zhang, M. Zhao, Microtubule assembly affects bone mass by regulating both osteoblast and osteoclast functions: Stathmin deficiency produces an osteopenic phenotype in mice, J. Bone Miner. Res. 26 (2011) 2052–2067, https://doi.org/10.1002/jbmr.419.
[54] D.C. Richardson, J. Zentek, Nutrition and osteochondrosis, Vet. Clin. North Am. Small Anim. Pract. 28 (1998) 115–135, https://doi.org/10.1016/s0195-5616(98)50008-3.
[55] N.Z. Frantz, G.A. Andrews, M.D. Tokach, J.L. Nelssen, R.D. Goodband, J.M. DeRouchey, S.S. Dritz, Effect of dietary nutrients on osteochondrosis lesions and cartilage properties in pigs, Am. J. Vet. Res. 69 (2008) 617–624, https://doi.org/10.2460/ajvr.69.5.617.
[56] P. Hartnett, L. Boyle, B. Younge, K. O'Driscoll, The effect of group composition and mineral supplementation during rearing on measures of cartilage condition and bone mineral density in replacement gilts, Anim. J. MDPI. 9 (2019), https://doi.org/10.3390/ani9090637.
[57] M. Robles, C. Gautier, L. Mendoza, P. Peugnet, C. Dubois, M. Dahirel, J.-P. Lejeune, I. Caudron, I. Guenon, S. Camous, A. Tarrade, L. Wimel, D. Serteyn, H. Bouraima-Lelong, P. Chavatte-Palmer, Maternal nutrition during pregnancy affects testicular and bone development, glucose metabolism and response to Overnutrition in weaned horses up to two years, PLoS One 12 (2017) e0169295, , https://doi.org/10.1371/journal.pone.0169295.
[58] A.C. Green, T.J. Martin, L.E. Purton, The role of vitamin a and retinoic acid receptor signaling in post-natal maintenance of bone, J. Steroid Biochem. Mol. Biol. 155 (2016) 135–146, https://doi.org/10.1016/j.jsbmb.2015.09.036.
[59] J.A. Williams, N. Kondo, T. Okabe, N. Takeshita, D.M. Pilchak, E. Koyama, T. Ochiai, D. Jensen, M.L. Chu, M.A. Kane, J.L. Napoli, M. Enomoto-Iwamoto, N. Ghyselinck, P. Chambon, M. Pacifici, M. Iwamoto, Retinoic acid receptors are required for skeletal growth, matrix homeostasis and growth plate function in postnatal mouse, Dev. Biol. 328 (2009) 315–327, https://doi.org/10.1016/j.ydbio.2009.01.031.
[60] C. Kruger, C. Talmadge, C. Kappen, Expression of folate pathway genes in the cartilage of Hoxd4 and Hoxc8 transgenic mice, Birth Defects Res. Part A - Clin. Mol. Teratol. 76 (2006) 216–229, https://doi.org/10.1002/bdra.20245.
[61] E. Feigerlova, L. Demarquet, J.-L. Guéant, One carbon metabolism and bone homeostasis and remodeling: a review of experimental research and population studies, Biochimie. 126 (2016) 115–123, https://doi.org/10.1016/j.biochi.2016.04.009.
[62] W. Laenoi, M.J. Uddin, M.U. Cinar, C. Phatsara, D. Tesfaye, A.M. Scholz, E. Tholen, C. Looft, M. Mielenz, H. Sauerwein, K. Schellander, Molecular characterization and methylation study of matrix gla protein in articular cartilage from pig with osteochondrosis, Gene. 459 (2010) 24–31, https://doi.org/10.1016/j.gene.2010.03.009.
[63] A.J. van Wijnen, J.J. Westendorf, Epigenetics as a new frontier in Orthopedic regenerative medicine and oncology, J. Orthop. Res. 37 (2019) 1465–1474, https://doi.org/10.1002/jor.24305.
[64] M. Weise, S. De-Levi, K.M. Barnes, R.I. Gafni, V. Abad, J. Baron, Effects of estrogen on growth plate senescence and epiphyseal fusion, Proc. Natl. Acad. Sci. U. S. A. 98 (2001) 6871–6876, https://doi.org/10.1073/pnas.121180498.
[65] A.E. Börjesson, M.K. Lagerquist, S.H. Windahl, C. Ohlsson, The role of estrogen receptor α in the regulation of bone and growth plate cartilage, Cell. Mol. Life Sci. 70 (2013) 4023–4037, https://doi.org/10.1007/s00018-013-1317-1.
[66] Y.-R. Jin, J.P. Stohn, Q. Wang, K. Nagano, R. Baron, M.L. Bouxsein, C.J. Rosen, V.A. Adarichev, V. Lindner, Inhibition of osteoclast differentiation and collagen antibody-induced arthritis by CTHRC1, Bone. 97 (2017) 153–167, https://doi.org/10.1016/j.bone.2017.01.022.
[67] S. Takeshita, T. Fumoto, K. Matsuoka, K. Park, H. Aburatani, S. Kato, M. Ito, K. Ikeda, Osteoclast-secreted CTHRC1 in the coupling of bone resorption to formation, J. Clin. Invest. 123 (2013) 3914–3924, https://doi.org/10.1172/JCI69493.
[68] F.J. Guo, Z. Xiong, X. Han, C. Liu, Y. Liu, R. Jiang, P. Zhang, XBP1S, a BMP2-inducible transcription factor, accelerates endochondral bone growth by activating GEP growth factor, J. Cell. Mol. Med. 18 (2014) 1157–1171, https://doi.org/10.1111/jcmm.12261.
[69] Y. Liu, J. Zhou, W. Zhao, X. Li, R. Jiang, C. Liu, F.J. Guo, XBP1S associates with RUNX2 and regulates chondrocyte hypertrophy, J. Biol. Chem. 287 (2012) 34500–34513, https://doi.org/10.1074/jbc.M112.385922.
[70] X. Han, J. Zhou, P. Zhang, F. Song, R. Jiang, M. Li, F. Xia, F.J. Guo, IRE1α dissociates with BiP and inhibits ER stress-mediated apoptosis in cartilage development, Cell. Signal. 25 (2013) 2136–2146, https://doi.org/10.1016/j.cellsig.2013.06.011.
[71] L. He, T. He, S. Farrar, L. Ji, T. Liu, X. Ma, Antioxidants maintain cellular redox homeostasis by elimination of reactive oxygen species, Cell. Physiol. Biochem. 44 (2017) 532–553, https://doi.org/10.1159/000485089.
[72] M.J. Coon, CYTOCHROME P450: Nature's Most versatile biological catalyst, Annu. Rev. Pharmacol. Toxicol. 45 (2005) 1–25, https://doi.org/10.1146/annurev.pharmtox.45.120403.100030.
[73] C. Tonelli, I.I.C. Chio, D.A. Tuveson, Transcriptional regulation by Nrf2, Antioxid. Redox Signal. 29 (2018) 1727–1745, https://doi.org/10.1089/ars.2017.7342.